Physico-chemical and mineralogical characterization of clay materials suitable for production of stabilized compressed earth blocks

Philbert Nshimiyimana [1, 2], Nathalie Fagel [3], Adamah Messan [1],
Dominique Osomba Wetshondo [4], Luc Courard [2]

[1] Institut International d'Ingénierie de l'Eau et de l'Environnement (Institut 2iE), Laboratoire Eco-Matériaux et Habitats Durables (LEMHaD), Rue de la Science, 01 BP 594 Ouagadougou 01, Burkina Faso

[2] Université de Liège (ULiege), Urban and Environmental Engineering (UEE), Allée de la Découverte 9, 4000 Liège, Belgium

[3] Université de Liège (ULiège), Argiles, Géochimie et Environnements sédimentaires (AGEs), Département de Géologie, Allée du 6 Août 14, 4000 Liège, Belgium

[4] Université de Kinshasa (UniKin), Département de Géosciences, B.P 190 Kin XI, Kinshasa, RD Congo

Abstract

The main objective of this study is to characterize the physico-chemical and mineral properties of clay materials from Burkina Faso to produce stabilized compressed earth blocks (CEBs). The reactivity of the clay materials was tested based on the electrical conductivity of solutions and the compressive strength of CEBs stabilized with 0-20 wt% CCR (calcium carbide residue) and cured for 45 days at 40±2 °C. Pabre and Kossodo respectively contain the highest fractions of clay (20-30%) and gravel (40%). Saaba and Pabre contain the highest content of kaolinite (60-70%) and quartz (45-60%) and recorded the highest and lowest reactivity, respectively. The compressive strength of CEBs stabilized with 20% CCR improved tenfold (0.8 to 8.3 MPa) for Saaba and only

2.6 (2 to 7.1 MPa) for Pabre. The clay materials in the present study are suitable to produce CCR-stabilized CEBs for load-bearing construction.

Keywords: Calcium carbide residue; clay material; compressed earth block; compressive strength; kaolinite; reactivity.

1. Introduction and background

Clay materials for application in construction of modern buildings have been mostly studied for production of fired products such as tiles and bricks [1-5]. The firing process is energy consuming and therefore not environmental-friendly, resulting in relative increase of the cost and embodied energy of the products [6-8]. Today, the awareness of the global warming and necessity for energy saving on the one hand and improved indoor comfort provided by unfired clay material on the other hand give this material the potential for construction of sustainable buildings [7,9-12]. For centuries, unfired clay materials have been used in building construction, in various forms such as adobe (sun dried brick), rammed earth and recently compressed earth block (CEBs), and proved promising to provide affordable and comfortable housing [7-10].

Burkina Faso is experiencing drastic demographic increase mainly in Ouagadougou, the capital city of 1.9 million inhabitants [13]. The valorization of local and non-conventional materials in modern construction can potentially contribute to providing the shelter to this population. Historically, the city of Ouagadougou is known to have been constructed using adobe and other techniques based on unfired clays. Clay materials lost much interest and acceptance with the arrival of so called “modern” materials such as cement and steel [14]. Clay materials from this region are basically used for road pavement and in some cases for the artisanal production of adobe; although some small enterprises such as Zi-Matériau and CC3D offer services of production, commercialization and construction with CEBs in the major cities. In fact, current research on

earth for building construction in Burkina Faso mainly reports on adobes and only a limited number of studies are reported on CEBs [10, 11, 14, 24-26].

CEBs are the most accepted form of unfired clay materials for the construction of modern building [7,10,15,]. This is basically related to their low (ambient) temperature of curing and other advantages such as improved mechanical and hygrothermal performances and durability, regular shape and size which allow to achieve various architectural designs contrary to the adobe and cement blocks [10, 15, 16, 18]. Clay material used for production of CEBs should have a certain fraction of fine particles and plasticity for binding cohesion of coarser particles in order to ensure physical and mechanical stability of the matrix, i.e. 10-50% of clay particles and plasticity index of 10-30, depending on the presence, the type and the content of stabilizer [7,9,12,16]. Table 1 presents the texture, plasticity, and mineralogy of earthen materials recommended for the production of stabilized CEBs. The CEBs should generally have dry compressive strength of at least 2 MPa for usage in non-load bearing walls, as prescribed by various standards and normative documents applicable in different parts of the world [15,18]. Nevertheless, the performances of the CEBs become critical when it comes to construction of load bearing walls and usage in water saturated conditions [7,12].

Table 1. Some recommendations for production of stabilized CEBs: texture, plasticity, mineralogy, type and content of stabilizer and physico-mechanical performances.

Parameters	Chemical stabilizers (mass percent)	
	Cement (5-10 %)*, a, c, f	Lime (6-12 %)*, a, c
Composition of the clay materials		
Clay particle (%) c, f	10-30	30-50
Plasticity index (%) c	10-20	20-30
Mineralogy **, c, e	Inactive	Active
Production and curing of stabilized CEBs		
Moisture of production (%) ***, a, b	10-15	15-20
Curing time in ambient condition (days) a	28	>28 (up to many months)
Physico-mechanical performances of cured CEBs		
Bulk density (kg/m^3) b	1600-2200	1400-2000
Dry compressive strength (MPa) b, c, d	4-12	2-7

Structural categories: Compressive strength of ordinary CEBs used in dry environment (CEB O D) according to ARS 673:1996 & ARS 674:1996 [g].	
CEB O 1 D: ≥ 2 MPa for no load-bearing applications (single-storey building).	
CEB O 2 D: ≥ 4 MPa for load-bearing applications in two-storey building.	
CEB O 3 D: ≥ 6 MPa for load-bearing applications in three-storey building.	
References	[a] [6-7], [b] [9,12], [c] [16], [d] [17], [e] [19], [f] [20], [g] [21], [22-23]

* Mass percentage of the dry mass of the clay materials.
** Inactive: no swelling minerals such as kaolinite, quartz.
** Active: swelling/ reactive minerals such as smectite (montmorillonite), poorly ordered kaolinite.
*** Mass percentage of the dry mass of clay material + stabilizer, at normal compaction pressure (1-2 MPa). The moisture content of production of CEBs can widely vary around the optimum moisture content dependent on the type of the clay material and stabilizer, thus need to be determined accordingly.
ARS(O): African regional standard (organization).

Many efforts have been made to improve the physico-mechanical performances of CEBs in dry and saturated conditions as well as their long term durability. This is mainly achieved by stabilization with chemical binders such cement, lime, geopolymer as well as by-product materials [6-7,15,18,24-26]. The stabilization of CEBs with by-product materials in partial or full substitution to classic binders not only improves the technical performance but also can potentially improve the sustainability and economic benefits of stabilized CEBs [8,24,27-28]. The compressive strength of CEBs, considered as an appropriate indicator of the mechanical performance of stabilized CEBs, should be at least 4 MPa and 2 MPa, respectively, in dry and saturated conditions for usage in the construction of load-bearing walls [7,15,21].

Prior studies used cement (5-10%) and lime (6-12%) to stabilize sandy (10-30 % clay particles, 10-20 of PI) and clayey (30-50 % clay particles, 20-30 of PI) earthen materials for production of CEBs, respectively [6,17,20,17,23]. The stabilization resulted in substantial improvement of the compressive strength of CEBs in dry and saturated conditions (Table 1). The improvement of the compressive strength was related to the formation of cementitious products such as calcium silicate hydrates (CSH) and calcium aluminate hydrates (CAH), either from the hydration reaction of cement or pozzolanic reaction between lime and aluminosilicate minerals such as kaolinite and fine particles of quartz (<50 µm) in the clay material [6,19,29,30-31]. More recently, calcium carbide residue (CCR), an industrial by-product rich in lime ($Ca(OH)_2$), showed the potential to

improve the compressive strength of CEBs through the chemical interactions with the clayey earthen material [24,26]. Therefore the suitability of clay materials should be characterized prior to the production of stabilized CEBs given that their performance is largely influenced by the characteristics of the earthen material, type and content of stabilizer as well as the production and curing process. Most of the studies focused on the textural and plasticity properties for selecting the appropriate clay materials for production of stabilized CEBs. Nevertheless, the latter chemical interactions prompted a further need for understanding the contribution of chemical/mineral composition of the clay materials on the performance of stabilized CEBs.

The present study investigates the suitability of clay materials from four different sites for the production of CCR-stabilized CEBs. This is achieved through the characterization of the physico-chemical and mineral properties of the clay materials and their reactivity. The effect of the mineral composition of the clay materials on their reactivity with CCR was evaluated based on the rate of consumption of calcium ions. The bulk density and compressive strength of CCR-stabilized CEBs were considered as the main criteria for selecting the most appropriate materials for construction of at least two-storey buildings.

2. Material and methods

2.1. Clay material

The study was carried out on clay materials from four different sites in the vicinity of Ouagadougou-Burkina Faso, i.e. Kamboinse, Pabre, Kossodo and Saaba (Fig. 1). The number of samples collected from each site depended on its size, exploitability and apparent variability.

The site of Kamboinse (K) is located 15 km in the North of Ouagadougou (12°29'24.48" N; 1°32'59.28" W; altitude 326 m). It has an average area of 700x200 m² and average thickness of exploitable layer of 6 m. The clay material from Kamboinse has a reddish-brown color, with some

whitish irregularities. The apparent texture of the particles varies depending on the depth: gravelly on the surface layer (< 2 m of depth), clay in the middle (2-6 m) and sandy in the depth (> 6 m) (Fig. 1). Pabre (P) is located 20 km in the North of Ouagadougou (12°31'23.46" N; 1°34'22.8" W; Alt. 297 m). It has an average area of 600x100 m² and thickness of exploitable layer estimated at 2 m. The clay material from Pabre was collected 50 cm under the top layer and has a silty clay texture (Fig. 1). This material has a grey color and is used for artisanal production of adobe bricks. Kossodo (Ko) is located 10 km in the North-East of Ouagadougou (12°27'49.32" N; 1°26'34.02"; W Alt. 303 m) and extends over an average area of 350x150 m² and has an average thickness of exploitable layer of 5 m. The clay material from Kossodo has a reddish-brown color, gravel-like texture on the top (depth ~3 m), silty-sandy texture in the depth (Fig. 1). The clay material from this site is used for production of cement stabilized CEBs by a local enterprise. Saaba (S) is located 15 km in the East of Ouagadougou (12°22'48.12" N; 1°24'2.22" W Alt. 310 m) and extends over an average area of 350x70 m² and has an average thickness of exploitable layer of 4 m. It is characterized by whitish a purple-brown clay material, which has sandy silt texture (Fig. 1). The clay materials from Saaba are exploited by the local population for artisanal production of construction materials and pottery.

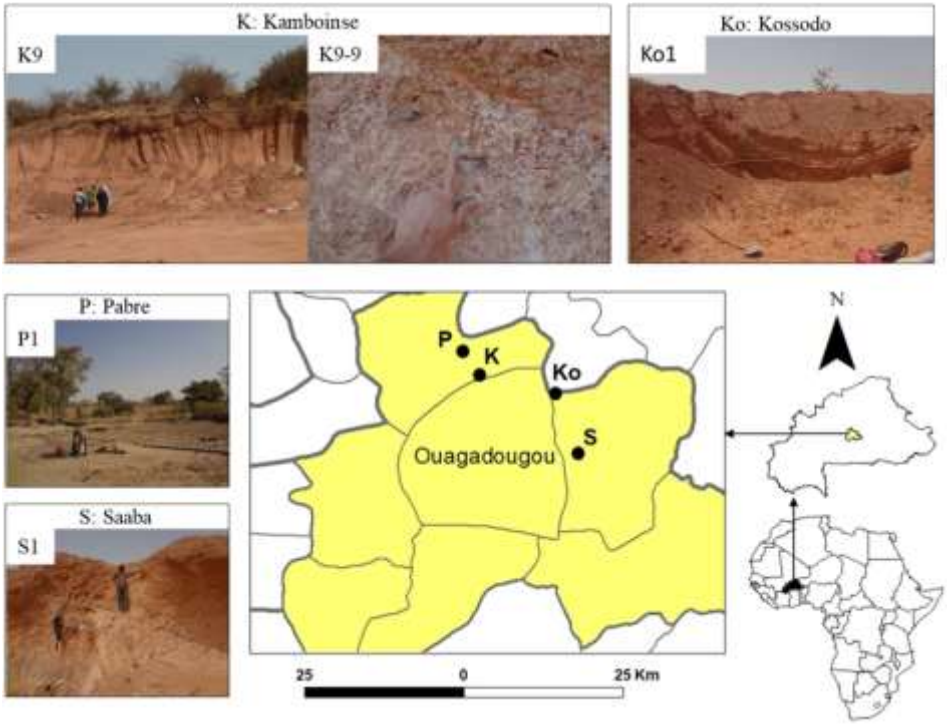

Fig. 1. Geographical setting of the Centre region of Burkina Faso and some views of the studied outcrops.

Table 2 presents the quantity of exploitable clay materials given the total volume of the deposit estimated from average dimensions (area and depth) of the deposit and volume of material already excavated from the deposit. Kamboinse contains the largest quantity of exploitable clay materials (700 000 m^3) while Saaba contains the smallest quantity (49 000 m^3).

Table 2. Average resources and samples of the clay materials from the four investigated sites.

Sites	Average length (m)	Average width (m)	Average depth (m)	Total volume (m^3)	Excavated volume (m^3)	Exploitable volume (m^3)
Kamboinse (K)	700	200	6	840 000	140 000	700 000
Pabre (P)	600	100	2	120 000	-	120 000
Kossodo (K)	350	150	5	262 500	131 250	131 250
Saaba (S)	350	70	4	98 000	49 000	49 000

Samples	Geographical coordinates on the surface	Depth (m)	Sample description (Rock color chart)
K1-3	12°29'24.48" N; 1°32'59.28" W; 326 m	3.5	Reddish brown (10R 4/6)
K3-1	12°29'32.76" N; 1°32'55.62" W; 315 m	2.5	Reddish brown (10R 4/6)
K3-2		3.5	Reddish brown (10R 4/6)
K3-4		3.5	Whitish orange (10 YR 8/2)
K3-5		5	Yellowish orange (10YR 8/6)
K4-1	12°29'32.4" N ; 1°32'52.44" W; 313 m	6.5	Reddish grey (5YR 8/1)
K4-2		6.5	Reddish brown (10R 4/6)
K4-3		5.5	Reddish brown (10R 4/6)
K4-4		7.5	Rose-grey (5YR 8/1)
K5-1	12°29'23.46" N ; 1°32'58.8" W; 321 m	5	Reddish brown (10R 4/6)
K5-2		4	Reddish brown (10R 4/6)

K5-3		3.5	Greyish orange (10YR 7/4)
K5-4		6	Greyish orange (10YR 7/4)
K6	12°29'17.88"N; 1°32'59.28"W; 310 m	1	Greyish orange (10YR 7/4)
K8	12°29'15.54" N; 1°33'2.4"W; 318 m	4	Reddish brown (10R 4/6)
K9-1	12°29'23.46" N ; 1°33'2.88"W; 328 m	1.5	Reddish brown (10R 4/6)
K9-2		3	Pale brown (5YR 6/4)
K9-3		3.5	Pale brown (5YR 6/4)
K9-4		4.5	Pale brown (5YR 6/4)
K9-5		5.5	Pale brown (5YR 6/4)
K9-6		6.5	Pale brown (5YR 6/4)
K9-7		7.5	Dark red-brown (10R 3/4)
K9-8		8.5	Pale orange (10 YR 8/2)
K9-9		9	Red (5R 5/4)
K9-10		3.5	Pale rose grey (5YR 8/1)
K9-11		5.5	Pale orange (10 YR 8/2)
P1	12°31'35.7" N; 1°34'31.5"W; 299 m	0.5	Yellowish brown (10YR 6/2)
P2	12°31'23.46" N; 1°34'22.8"W; 297 m	0.5	Yellowish brown (10YR 6/2)
P3	12°31'18.36" N; 1°34'18"W; 293 m	0.5	Yellowish brown (10YR 6/2)
Ko1-1	12°27'49.32" N; 1°26'34.02" W; 303 m	2.9	Brown gravel-like
Ko1-2		3.1	Pale brown silty clayey (5YR 5/6)
Ko1-3		3.9	Pale brown silty clayey (5YR 5/6)
Ko1-4		4.9	Dark yellowish orange silty clayey (10YR 6/6)
S1-1	12°22'44.88" N ; 1°24'38.1" W; 315 m	2.3	Reddish brown (10R 4/6)
S1-2		3.9	Rose orange (10R 7/4)
S1-3		4	Pale red (5R 6/2)
S1-4		4.5	Rose grey (5YR 8/1)
S1-5		5	Pale red (5R 6/2)
S2-1	12°22'48.12" N; 1°24'2.22"W; 310 m	0.75	Greyish orange (10R 8/2)
S3-1	12°22'44.04" N; 1°24'34.08"W; 312 m	4	Greyish orange (10R 8/2)
S3-2		4.5	Reddish brown (10R 5/4)

2.2. Calcium carbide residue

Calcium carbide residue (CCR) is whitish-grey by-product material formed from the hydrolysis of calcium carbide (CaC_2) during the production of acetylene gas. It was collected from Burkina Industrial Gas (BIG) in Ouagadougou, ground and sieved to a particle size of 125 µm. Prior study reported that the CCR contains up to 43 % lime ($Ca(OH)_2$), determined by mean of X-ray powder diffraction and thermogravimetric analysis, has a median particle size (D_{50}) of 20.5 µm and can improve the compressive strength of CEBs [24].

2.3. Physico-chemical and mineral characterization of the clay material

Particle size distribution (PSD), clay: <0.002 mm, silt: 0.002-0.08 mm, sand: 0.08-2 mm and gravel: >2 mm, was determined referring to NF EN ISO 17892-4 standards [32]. Atterberg's plasticity limits (liquidity and plasticity) were determined using a Casagrande apparatus in

accordance with NF P 94-051 [33]. The specific density of particles was determined according to NF EN 1097-6 [34]. The optimum water content required for achieving the maximum dry density was determined by standard proctor test according to NF P 94-093 [35]. These physical and geotechnical properties were characterized at the laboratory LEMHaD, 2iE, Burkina Faso.

Chemical composition was analyzed by means of X-Ray Fluorescence (XRF) technique using ARL Perform'X Sequential XRF equipment (Department of geology, PGEP, ULiege, Belgium). After determination of loss-on-ignition at 1000 °C for 2 hours (LOI 1000), about 340-450 mg (Ms) of the sample were fused in lithium borate (11xMs) to form pellets. The major chemical elements were determined on the pellets against an internal standard calibrated from sodium to uranium.

Mineral composition was analyzed by X-Ray diffraction (XRD) performed using the Bruker D8-Advance Eco 1.5 kW diffractometer equipped with copper anticathode (Cu Kα λ=1.54060 Å at 40 kV and 25 mA) and Lynxeye xe detector (Department of geology, AGEs, ULiege, Belgium). The bulk mineralogy was identified by powder diffraction on samples ground to less than 150 µm, while the clay minerals were identified on oriented <2 µm aggregates throughout treatments (air-drying, glycolated and heat treatment). The XRD patterns were acquired from 2 to 70° 2θ, at step size of 0.02° 2θ, scan time of 2 s per step for bulk samples and 2 to 30° 2θ, step size of 0.009° 2θ, scan time of 0.5 s per step for oriented aggregates. The acquired patterns were analyzed using Diffrac.Eva V4.11 software of Bruker. The mineral composition was further confirmed by thermogravimetric analysis (TGA) and Fourier Transform Infrared Spectroscopy (FTIR). The TGA was carried out using automatic multiple sample thermogravimetric analyzer TGA-2000 of the Las Navas Instruments (Department of Geology, AGEs, ULiège, Belgium). The analysis was carried out in 25-1000 °C range at a heating rate of 5 °C/min in dry air environment. FTIR was recorded using FTIR spectrometer in the range of 4000-400 cm^{-1} at scan size of 1 cm^{-1} (Department of ArGenCo, UUE, ULiège, Belgium). The FTIR was carried out on pellets formed using 2 g of the clay materials (ground to <250 µm) and 148 g of potassium bromide.

Semi-quantitative estimation of the mineral composition was achieved based on the measurement of the intensity of diagnostic peaks of minerals identified by XRD on which corrective factors were applied, i.e. “XRD: Method A”, according to [36-38]. The content of kaolinite and goethite were confirmed based on the mass loss on the TGA due to their respective dehydroxylation compared to that of pure kaolinite (13.97% at 530-590°C) and pure goethite (10.13% at 290-330°C), i.e. “TGA: Method B” [2,39]. Additionally, the mineral composition was estimated based on chemical analysis by XRF and applying the formula proposed by [40] in [2]. This so-called “XRF: Method C” allows assigning different oxides to minerals identified by XRD and TGA. The following assignments were made: (1) K_2O to illite or K-feldspar, (2) CaO to plagioclase, (3) Al_2O_3 to kaolinite after subtracting the contribution to illite or K-feldspar, (4) SiO_2 to quartz after subtracting the contribution to illite or K-feldspar and kaolinite, (5) Fe_2O_3 to hematite after subtracting the contribution to goethite (determined from the TGA). The values of the mineral composition obtained from “Method A” and “Method C” were normalized with respect to 100 %.

$$\%\text{illite} = \frac{K_2O}{94}814 \quad \text{or} \quad \%\text{K-feldspar}\frac{K_2O}{94}557 \tag{1}$$

$$\%\text{plagioclase} = \frac{CaO}{56}278 \tag{2}$$

$$\%\text{kaolinite} = \frac{\%Al_2O_3 - \frac{\%\text{illite x } 102x3}{814} - \frac{\%\text{K-feldspar x}102}{557} - \frac{\%\text{plagioclase x } 102}{278}}{102}258 \tag{3}$$

$$\%\text{quartz} = \frac{\%SiO_2 - \frac{\%\text{illite x } 60\text{ x}6}{814} - \frac{\%\text{K-feldspar x } 60\text{ x } 6}{557} - \frac{\%\text{plagioclase x } 60\text{ x } 2}{278} - \frac{\%\text{kaolinite x } 60\text{ x } 2}{258}}{60}60 \tag{4}$$

$$\%\text{hematite} = \frac{\%Fe_2O_3 - \frac{\%\text{goethite x } 160}{178}}{160}160 \tag{5}$$

814= molar mass of illite $(K_2O)(SiO_2)_6(Al_2O_3)_3(H_2O)_3$ in g/mol

557= molar mass of K-feldspar $(K_2O)(SiO_2)_6(Al_2O_3)$ in g/mol

278= molar mass of plagioclase $(CaO)(SiO_2)_2(Al_2O_3)$ in g/mol

258= molar mass of kaolinite $(SiO_2)_2(Al_2O_3)(H_2O)_2$ in g/mol

94= molar mass of K_2O in g/mol

56= molar mass of CaO in g/mol

102= molar mass of Al_2O_3 in g/mol

60= molar mass of SiO_2 in g/mol

60= molar mass of quartz (SiO_2) in g/mol

160= molar mass of Fe_2O_3 in g/mol

178= molar mass of goethite (Fe_2O_3)(H_2O) in g/mol

2.4. Tests of the suitability of clay material

The suitability of different clay materials for the production of stabilized CEBs was tested based on the rate of reactivity with the CCR and physico-mechanical performances of CEBs stabilized with CCR. The evaluation of the reactivity aims to estimate the initial content of the CCR required by the clay material for the pozzolanic reactivity to take place and monitor the rate of consumption of that CCR over the curing time. It was assessed based on the evolution of the pH and electrical conductivity (EC) in the mix solutions made of clay materials and CCR, referring to [26].

The representative clay materials from different sites, i.e. the mix of samples from different point on each site, were washed on 400 µm to collect the undersize and dried at 40±2 °C. The finer fraction of clay materials, undersize on 400 µm, was considered for their binding and reactivity contribution to the earthen materials contrary to the coarser fraction. Dry mixtures were prepared using 5 g of dry clay material and 0, 10, 20 wt% CCR (mass percent of CCR with respect to the dry mass of the clay materials). The dry mixtures were completed with 200 mL of distilled water to prepare mix solutions. Mix solutions were cured for 1 to 45 days at 40±2°C in tightly closed bottles to minimize carbonation. The initial pH and EC were measured after different curing times (1, 14, 28 and 45 days) using pHenomenal MU 6100 L multiparameter lab conductimeter equipped with CO 11 conductivity probe and pH electrode.

CEBs stabilized with CCR were produced using clay materials from different sites and 0, 10, 20% CCR. The clay materials were sieved on 5 mm and dry mixed with CCR until apparent homogeneity, as recommended by CRATerre [16]. The optimum amount of water, determined according to the static compaction method proposed by CDE [41] was added to the dry mix and mixed until homogeneous moisture distribution. An appropriate amount of humid mix was

manually compressed in a prismatic mold (295x140x95 mm^3) of a Terstaram press machine to mold the CEBs. The Terstaram machine allow to reach the compaction pressure up to 35 bars [25]. The CEBs were stored in polyethylene bags, to prevent the loss of humidity and eventual carbonation, and cured for 45 days in an oven at 40±2 °C. After the curing, the CEBs were dried at 40±2 °C until reaching constant mass (change of weigh less than 0.1 % for 24 hour). The compressive strength was tested on stack of two halves of the CEBs according to the XP P13-901 standard [42].

3. Results and discussion

3.1. Particle size distribution of the clay material

The particle size distribution (PSD) curves of the clay materials from different sites are presented in Fig. 2. These curves show continuous PSD for all samples, basically clay particles (<0.002 mm), silt (0.002-0.08 mm), sand (0.08-2 mm) and gravel (> 2 mm). The shape of the PSD curve varies for different sites and within the same site, for the case of Kamboinse. The clay materials from Pabre (Fig. 2a) and Saaba (Fig. 2d) have PSD fitting in the boundaries recommended by the CRATerre [16] for production of CEBs stabilized with lime. By contrast, Kossodo (Fig. 2c) does not fit within these boundaries, as well as some points from Kamboinse (Fig. 2b). However, it is noteworthy that these boundaries are just guidelines which do not have to be fully satisfied by the earthen materials [16].

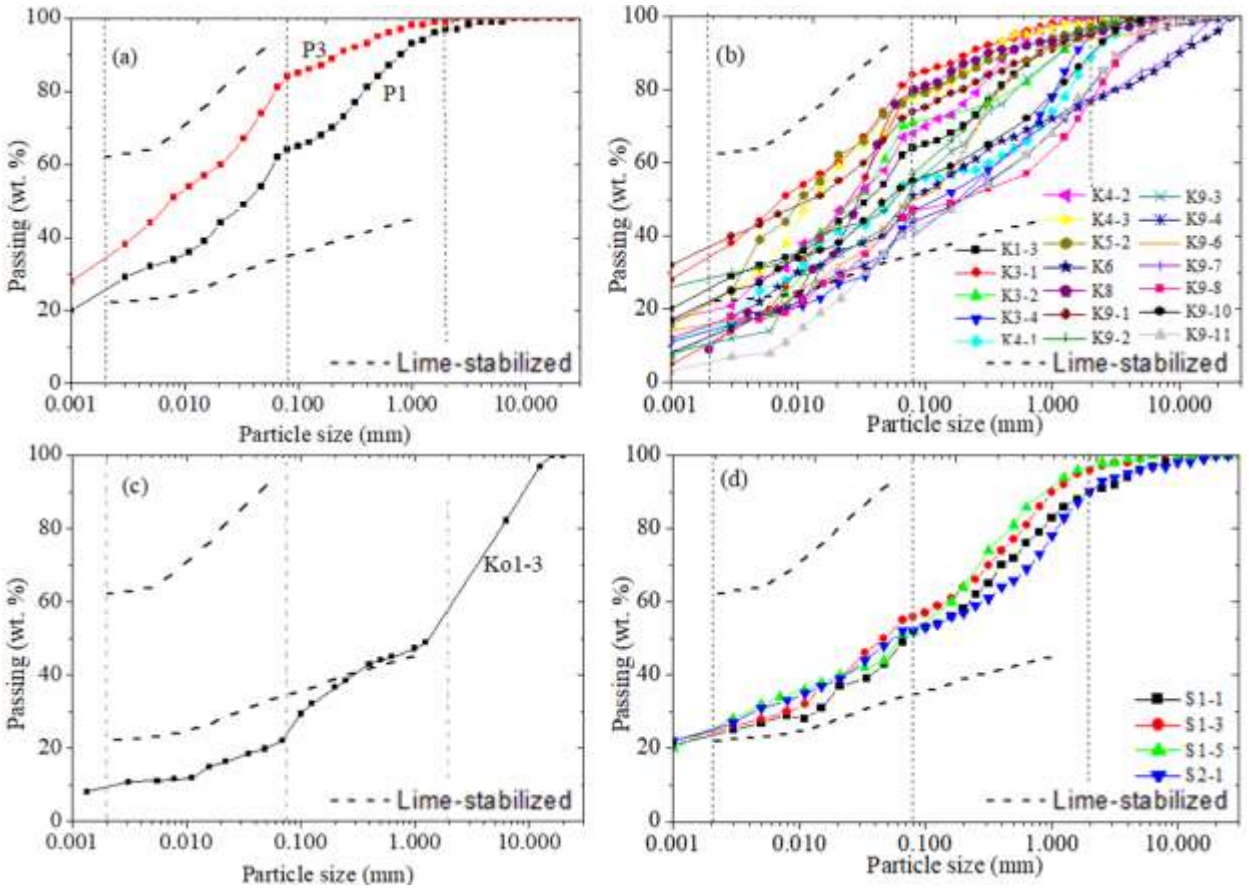

Fig. 2. Particle size distribution of the bulk samples from the four investigated sites: (a) P=Pabre, (b) K=Kamboinse, (c) Ko=Kossodo, (d) S=Saaba. Comparison with CRATerre boundaries recommended for lime stabilized earthen materials [16].

The variations of PSD of the clay materials from Kamboinse range in 10-25 % of clay particles except K3-1, K8, K11 and K9-1, K9-2 which respectively contain <10% and >25% of clay particles, 30-60 % of silt, 15-45 % of sand and 0-20 % of gravel (Fig. 3a). The PSD of the clay materials from Pabre is characterized by 20-30 % of clay particles, 40-55 % of silt, 15-35% of sand and 0-5 % of gravel (Fig. 3b).The sample analyzed from Kossodo contained less than 10% of clay particles, 15 % of silt, 35 % of sand and 40 % of gravel (Fig. 3c). The materials from Saaba contained 20-25 % of clay, 25-30 % of silt, 40-45 % of sand and less than 10 % of gravel (Fig. 3d).

Samples from Pabre contain the highest fraction of clay particles, while Kamboinse, Saaba and Kossodo respectively contain the highest fractions of silt, sand and gravel particles. In term of total fraction of fine particles (<0.08 mm: clay + silt), Pabre contains the highest fraction (60-85 %)

followed by Kamboinse (50-80 %), Saaba (~50 %) and Kossodo (~25 %). It is noteworthy that Saaba has relatively homogeneous PSD, while Kamboinse has the most heterogeneous PSD.

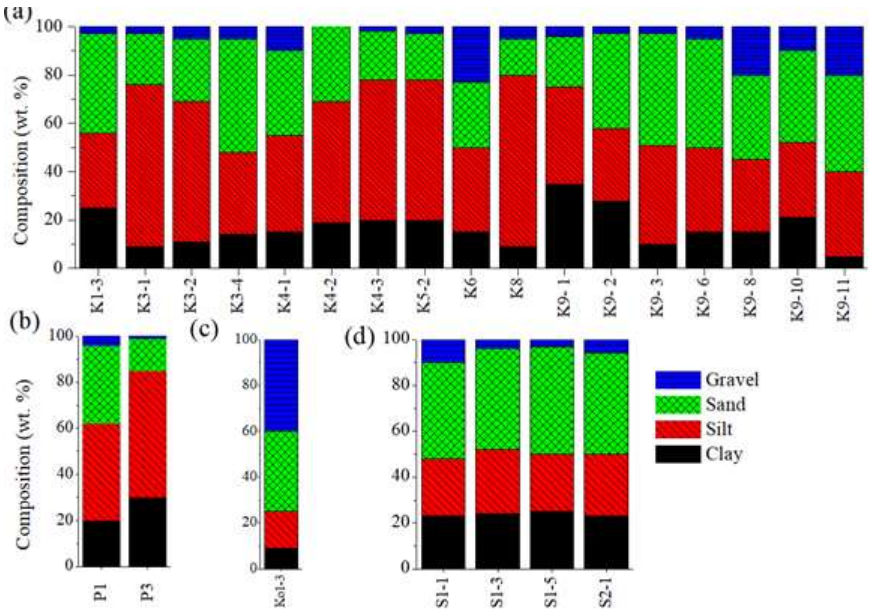

Fig. 3. Fractions of particle size of the bulk samples from the four investigated sites: (a) K=Kamboinse, (b) P=Pabre, (c) Ko=Kossodo, and (d) S=Saaba.

3.2. Plasticity of the clay materials

Fig. 4 presents the relationship between plasticity index (PI) and limit of liquidity (LL) of all samples. The plasticity behaviors vary from medium to high plastic silt (under the A-line) and medium to high plastic clay (above the A-line). The clay materials from Pabre are characterized by a PI of 20 and LL of 35-40 (Fig. 4a). The PI and LL of the clay materials from Kamboinse range in 10-25 and 40-65, respectively, except K3-1 and K8 (PI: 35, LL: 60) (Fig. 4b). The sample from Kossodo has a PI of 15 and LL of 40 (Fig. 4c). The clay materials from Saaba have a PI of 10-20 and LL of 45-55 (Fig. 4d). These results suggest that the clay materials from Pabre behave as clay of medium plasticity; those from Kamboinse and Saaba as silt-clay and silt of medium to high plasticity, respectively; Kossodo as silt-clay of medium plasticity.

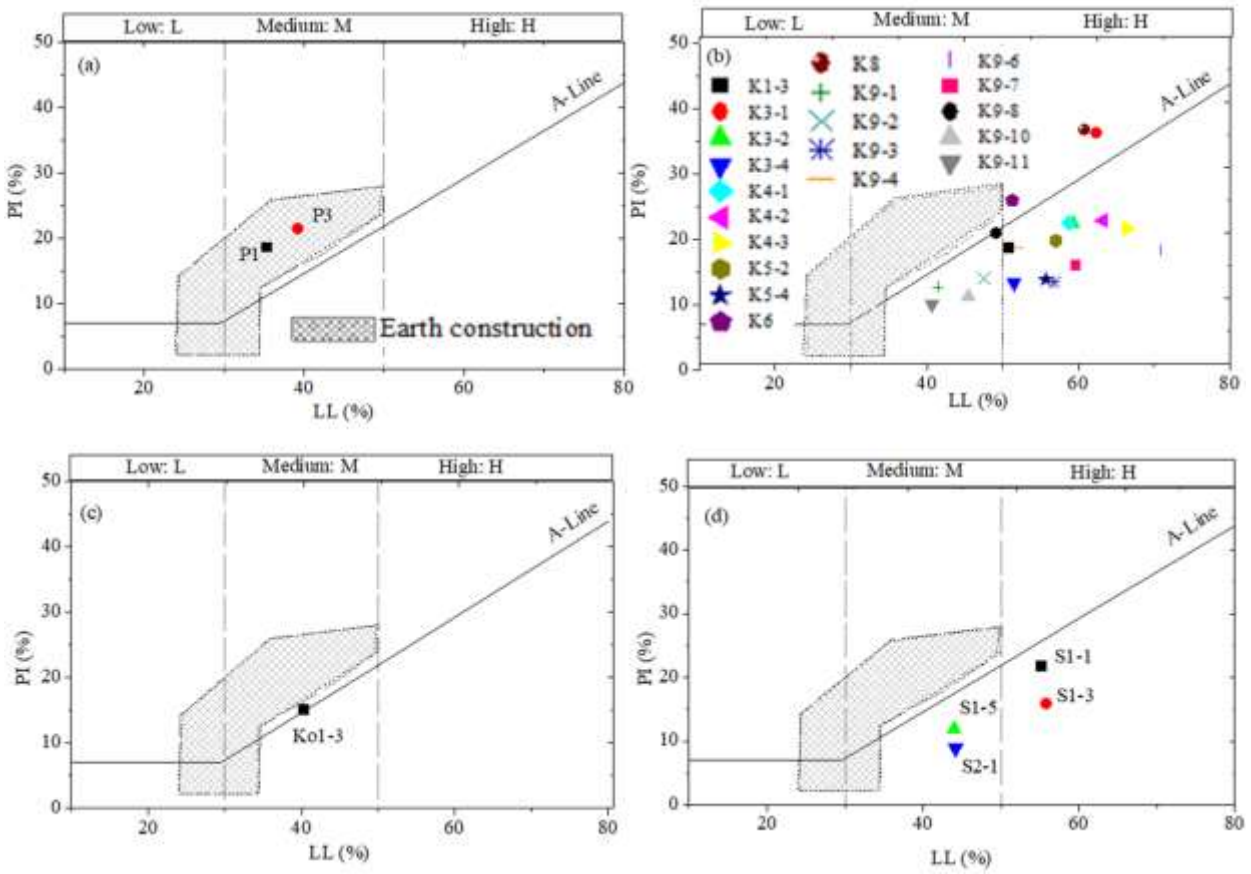

248

249 Fig. 4. Plasticity of the bulk samples from the four investigated sites: (a) P=Pabre, (b)
250 K=Kamboinse, (c) Ko=Kossodo, and (d) S=Saaba. Comparison with the boundaries recommended
251 for earthen construction [42].

252 The clayey behavior of the materials from Pabre (PI ≥ 20, LL > 30) agrees with their high content
253 of the fine particles (60-85% of clay + silt) and give them high cohesion. Similarly, clay materials
254 from Kamboinse have medium to high cohesion given their silt-clay behavior (PI of more or less
255 than 20 and LL > 30) and high fraction of fine particles (50-80%). Kossodo and Saaba, both having
256 PI < 20 and small fraction of fine particles (< 50%) have medium cohesion [16]. Moreover, clay
257 materials from Pabre and Kossodo have plasticity close to that recommended for earth construction
258 [42], thus they would be more suitable for production of unstabilized CEBs. Clay materials with
259 high cohesion and continuous PSD would be suitable for production of CEBs.

3.3. Chemical composition of the clay materials

The chemical composition of selected samples from different sites mainly consists of silica (SiO_2), alumina (Al_2O_3), iron (III) oxide (Fe_2O_3) and traces of CaO, MgO, Na_2O, K_2O (Table 3). The samples from Kamboinse, Kossodo and Saaba basically contain 40-60 % of silica, 20-30 % of alumina and 0-15 % of iron (III) oxide. The sample from Pabre (P1) contains the highest fraction of silica (~75 %) and the lowest fraction of alumina (~11 %) compared to other sites. The contents of oxides in samples from Kamboinse, Kossodo and Saaba are consistent with the chemical composition of kaolinite-rich clay minerals [5]. The occurrence of CaO, MgO, Na_2O, K_2O in trace reflects the unlikely presence of high swelling clay minerals such smectite [43].

The content of iron (III) oxide (0-15 %) can be related to the increasing reddish brown color which may suggest the presence of goethite. The ratio of SiO_2/Al_2O_3 generally varied between 2 to 3, apart from exceptional samples such as P1 (6.6), K3-1 (1.6) (Table 3). This ratio reveals the difference in mineral content, where the highest ratio can be related to the highest content of quartz and *vice versa* [2]. For most samples, the range of variation of the LOI 1000 between 9-12 % (at the exception of P1, LOI 1000 = 5.7 %) reveals the presence of mainly hydrated minerals such as clay and goethite [2]. High ratio of SiO_2/Al_2O_3 (>3) and low LOI 1000 (5.7 %) in the sample from Pabre (P1) suggests an important contribution of quartz and low content of clay minerals [2,4]. Moreover, Table 3 shows that the sum of SiO_2, Al_2O_3, and Fe_2O_3 is greater than 75 % which agrees with some recommendations for stabilized CEBs [12].

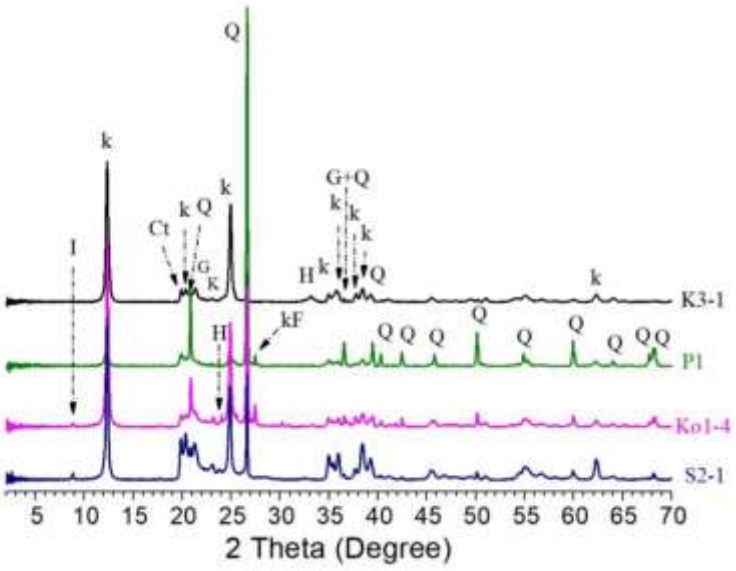

279

280 Fig. 5. XRD patterns of selected bulk samples from the four investigated sites. K=Kamboinse,
281 P=Pabre, Ko=Kossodo, S=Saaba; Ct= total clay, k= kaolinite, I= Illite, Q= quartz, kF=K-feldspar.

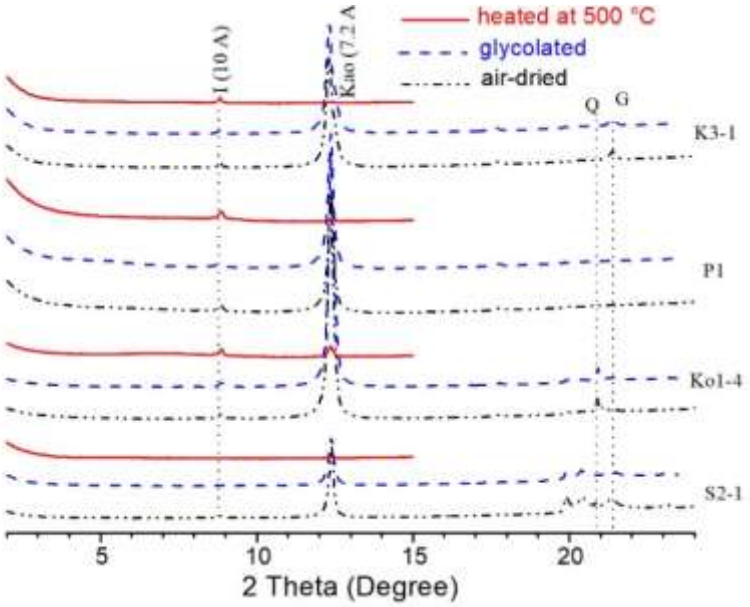

282

283 Fig. 6. XRD patterns of selected oriented aggregates from the four investigated sites:
284 K=Kamboinse, P=Pabre, Ko=Kossodo, S=Saaba; kao= kaolinite, I= illite, Q= quartz,
285 G= goethite.

286 **3.4. Mineral composition of the clay materials**

287 The XRD spectra of bulk samples selected from the four investigated sites mainly revealed the
288 diagnostic reflection of clay mineral (4.47 Å), kaolinite (7.15 Å), quartz (3.34 Å), goethite
289 (2.44 Å), hematite (2.69 Å) and traces of K-feldspars and illite (Fig. 5). The spectra of the oriented

aggregates confirmed the predominance of kaolinite and some traces of illite (Fig. 6). The reflection of kaolinite clay appeared at 7.15 Å on air-dried and glycolated samples and disappears on heating at 500 °C for 4 hours, while that of illite appeared at 10 Å and remained throughout all treatments [38].

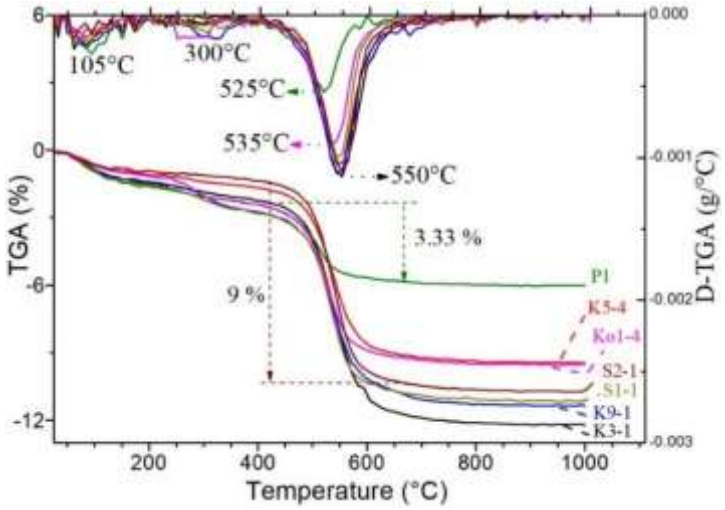

Fig. 7. Thermogravimetric analysis (TGA) and derivative thermogravimetric analysis (D-TGA) curves of bulk samples selected from the four investigated sites. K=Kamboinse, P=Pabre, Ko=Kossodo, S=Saaba.

Fig. 7 presents the thermogravimetric analysis (TGA) of samples selected from different sites. The samples recorded a loss of mass around 550 °C (i.e., between 450 and 650 °C) corresponding to the dehydroxylation of kaolinite [39]. At this temperature range, sample S2-1 recorded the highest loss of mass (9 %), while P1 recorded the lowest loss of mass (3.33 %). This confirms that S2-1 and P1 contain the highest and lowest fraction of kaolinite, respectively. The thermal removing of hydroxyl groups in kaolinite was previously reported around 530-590 °C, depending on the degree of crystallinity [2,39,43]. Early onset of the dehydroxylation can be related to poorly ordered structure of kaolinite [43]. The TGA/D-TGA displays the peak of dehydroxylation of kaolinite in samples P1 and Ko1-4 at lower temperature (525-535 °C) compared to other samples (550 °C) (Fig. 7). This suggests that the sample from Pabre not only contains the lowest content of kaolinite but also, similarly to Kossodo, this kaolinite is relatively poorly ordered.

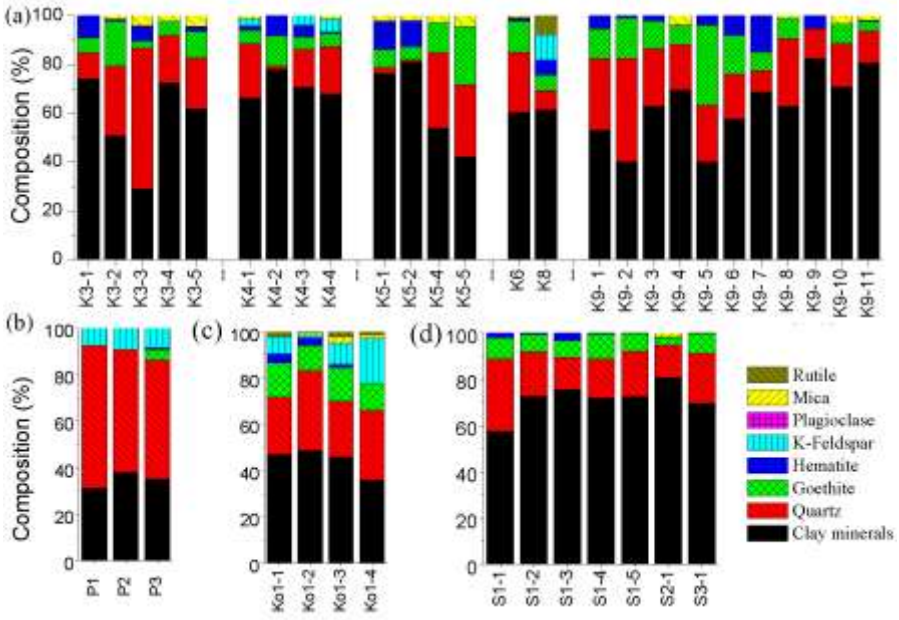

Fig. 8. Semi quantitative analysis of the bulk samples from the investigated sites estimated by XRD powder diffraction (i.e. method A). K=Kamboinse, P=Pabre, Ko=Kossodo, S=Saaba.

The semi-quantitative estimation of mineral composition of the bulk samples confirmed the predominance of clay minerals, quartz with minor goethite, hematite and K-feldspar and trace of mica, plagioclase and rutile (Fig. 8). The mineral composition widely varies from one site to another. The clay materials from Kamboinse contain 40-75 % of clay minerals, 5-40 % of quartz, 0-20 % of goethite, <10 % of hematite (Fig. 8a). Pabre contains 30-35 % of clay mineral, 45-60 % of quartz, <5 % of goethite, <5 % of hematite, and <10 % of K-feldspar (Fig. 8b). Kossodo is characterized by 35-50 % of clay mineral, 25-35 % of quartz <15 % of goethite, <5 % of hematite and <20 % of K-feldspar (Fig. 8c). Saaba contains 60-80 % of clay mineral, 15-30 % of quartz, <10 % of goethite and <5 % of hematite (Fig. 8d). Saaba is characterized by the highest content of clay mineral (60-80 %) and lowest content of quartz (15-30 %). By contrast, Pabre contains the lowest content of clay mineral (30-35 %) and highest fraction of quartz (40-60 %). Kamboinse and Kossodo have medium composition of clay mineral. The mineral composition of Kamboinse is the most heterogeneous among the investigated sites.

Table 3. Chemical and mineral composition of selected samples from the investigated sites.

Chemical composition of selected samples (%)								
Oxides		Kamboinse			Pabre	Kossodo	Saaba	
		K3-1	K5-4	K9-1	P1	Ko-4	S1-1	S2-1
SiO_2		42.9	63.7	49.7	76.9	55.0	53.5	60.9
Al_2O_3		27.3	23.3	24.0	11.7	23.4	24.7	27.6
Fe_2O_3		15.7	2.3	13.0	3.8	8.1	9.7	0.6
CaO		0.1	0.1	0.6	0.2	0.1	0.1	0.1
TiO_2		1.4	0.5	0.9	0.9	1.2	0.9	0.0
MnO		0.1	0.0	0.0	0.1	0.0	0.0	0.0
MgO		0.1	0.0	0.1	0.0	0.0	0.0	0.0
Na_2O		0.0	0.0	0.0	0.0	0.0	0.0	0.0
K_2O		0.1	0.3	0.2	0.8	2.3	0.1	0.1
P_2O_5		0.1	0.0	0.1	0.0	0.1	0.0	0.0
Total LOI (1000 °C for 2 hours)		12.1	9.7	11.3	5.7	9.8	10.9	10.6
Total oxides		100	100	100	100	100	100	100
SiO_2/Al_2O_3 ratio		1.6	2.7	2.1	6.6	2.4	2.2	2.2
$SiO_2 + Al_2O_3 + Fe_2O_3$		85.9	89.3	86.8	92.4	86.5	87.9	89.2
TGA mass loss: 200-400°C		-0.8	-0.6	-1.3	-0.8	-1.3	-1.3	-0.4
TGA mass loss: 450-650°C		-9.4	-7.3	-7.9	-3.4	-6.8	-7.9	-8.9
Mineral composition of selected samples (%)								
Methods	Minerals	K3-1	K5-4	K9-1	P1	Ko1-4	S1-1	S2-1
A: XRD (powder & oriented aggregate)	Quartz	11	31	29	61	30	31	14
	Goethite	6	12	12	0	12	9	3
	Hematite	9	0	5	0	0	2	0
	K-feldspar	0	0	0	8	19	0	0
	Plagioclase	0	0	0	0	0	0	0
	Mica	0	3	0	0	2	0	2
	Rutile	0	0	0	0	1	0	0
	Total clay minerals	74	54	54	31	36	58	81
	Clay minerals							
	Kaolinite	69	47	53	29	35	58	78
	Illite	5	7	1	2	1	0	3
	Total: Method A	100	100	100	100	100	100	100
B: TGA	Goethite (200-400°C)	8	6	13	8	12	12	4
	Kaolinite (450-650°C)	67	53	57	24	49	56	64
C: XRF (chemical analysis)	Illite	1	3	2			1	1
	K-feldspar				5	13		
	Plagioclase	1	1	3	1	1		
	Kaolinite	70	55	58	26	52	61	67
	Quartz	11	35	22	60	22	25	28
	Goethite	8	6	13	8	12	12	4
	Hematite	9		2		1	1	
	Total: Method C	100	100	100	100	100	100	100

Table 3 comparatively summarizes the chemical and mineral composition of selected samples from different sites using different methods. It shows that kaolinite is the main clay mineral accompanied by traces of illite (±5 %). The kaolinite content determined from TGA (Method B) is in good agreement (within ±5 %) with XRF (Method C), while the content estimated by XRD (Method A) differs up to ±10 %. Exceptionally for the sample Ko1-4 from Kossodo, the content of kaolinite significantly differs for XRD (35 %) and TGA/XRF methods (49/52 %). This

difference can be related to the possible disorder in the structure of kaolinite from Ko1-4, as suggested from the TGA, whereby the fraction of disordered kaolinite is not detected by XRD.

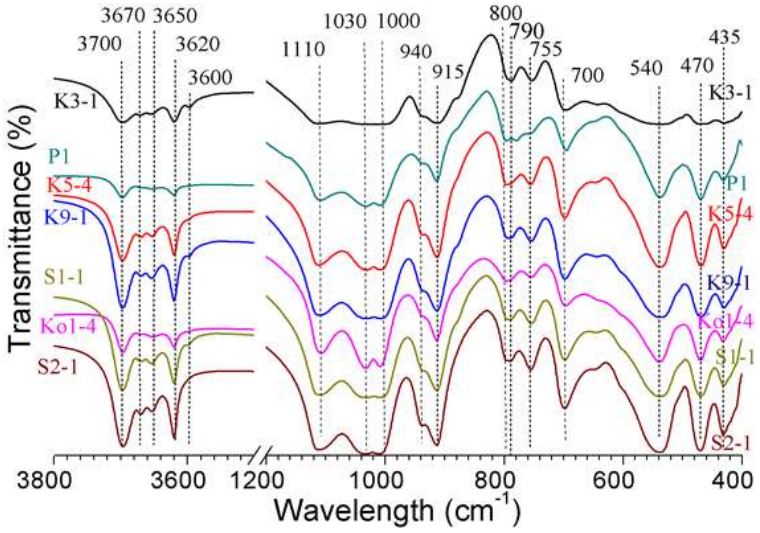

Fig. 9. FTIR spectra of bulk samples of clay materials selected from the investigated sites. K=Kamboinse, P=Pabre, Ko=Kossodo, S=Saaba.

The FTIR confirmed the predominance of kaolinite and quartz mineral (Fig. 9). Intense transmittance bands detected at 3700, 3670, 3652 and 3620 cm^{-1} are related to the stretching of hydroxyl groups in the kaolinite, while the mild band at 3600 cm^{-1} is related to the illite [45]. Bands at 1110, 1030 and 1000 cm^{-1} correspond to the vibration of Si-O bonds, those at 940 and 915 cm^{-1} to vibration of Al-OH bonds in the kaolinite as already observed by [5,43,45]. The bands at 790 and 755 cm^{-1} correspond to the vibration of Si-O-Al while those around 540 cm^{-1} and 470 cm^{-1} respectively correspond to the stretching of Si-O-Al and Si-O bonds of the kaolinite [45].

The bands in 3700-3620 cm^{-1} are useful for qualitative assessment of the structure of kaolinite in a sense that well-defined bands represent well-ordered kaolinite and the disappearance of the band at 3670 cm^{-1} represents poorly ordered kaolinite [5,43,45-46]. Samples K9-1 and K5-4 (from Kamboinse), S1-1 and S2-1 (from Saaba) present intense and well-defined diagnostic bands of kaolinite (3700-3620 cm^{-1}) while K3-1, P1 and Ko1-4 (from Kamboinse, Pabre and Kossodo,

respectively) recorded low intensities. The contents of kaolinite in samples K3-1, P1, and Ko1-4 estimated from the TGA are respectively 67 %, 24 % and 49 % (Table 3). This suggests that the disappearance of the bands at 3650 and 3670 cm^{-1} can be related not only to the low content of the kaolinite in P1 but also to the poor order of its structure in K3-1, P1 and Ko1-4. This is in agreement with the early onset of the dehydroxylation in P1 and Ko1-4 observed during TGA/D-TGA. The mild intensity of the vibration band at 940 cm^{-1} for K3-1 and Ko1-4 samples is also consistent with a poorly ordered clay mineral [5,43]. Additionally, the lack of well resolved bands at 1110-1000 cm^{-1} and 540 cm^{-1} in sample K3-1 suggests the presence of defects in Si-O and Si-O-Al bonds of the kaolinite. The occurrence of poorly ordered kaolinite would be beneficial for its reactivity during the pozzolanic reaction with lime [6,43-44,46].

3.5. Suitability of clay materials for production of stabilized compressed earth blocks

3.5.1. Initial pH and evolution of electrical conductivity of the mix solutions

The initial pH of the solutions of clay materials were 8.5 for Kamboinse, 6.1 for Pabre, 5.2 for Kossodo, and 5.5 for Saaba. The pH reached the apparent maximum values of 11.7 for Kamboinse, 11.4 for Pabre, 11.3 for Kossodo, and 11.4 for Saaba after 1 hour of addition of 2 % CCR compared to the pH of 11.6 for the solution of 2 % CCR alone. This suggests that at least 2 % CCR is necessary to satisfy the short term modification and increase the pH of all clay materials [26]. This is related to the predominance of low activity clay mineral, such as kaolinite, in all clay materials. Therefore, more than 2 % CCR would be necessary for triggering and sustaining the long term pozzolanic reaction in all clay materials [47].

Fig. 10 shows the evolution of the electrical conductivity (EC) of the mix solutions containing the clay materials and 10-20 % CCR over the curing time. Note that the EC of the solution of the clay materials alone remained less than 0.1 mS/cm over time, while that of the solutions of CCR alone was greater than 6.3 mS/cm. Fig. 10a and Fig. 10b show that the initial EC (after 1 hour) of the

clay materials mixed with 10 % and 20 % CCR respectively reached at least 5.8 mS/cm and 6.0 mS/cm. The dissolution of portlandite ($Ca(OH)_2$) from CCR into Ca^{2+} and OH^- was responsible for this drastic increase of the initial pH and EC [26,47].

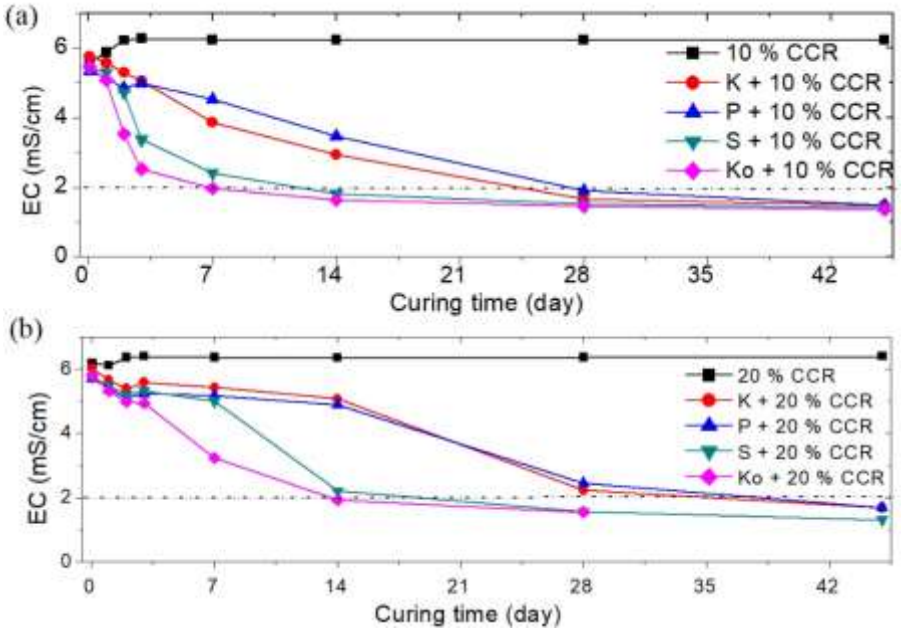

Fig. 10. Evolution of electrical conductivity (EC) in mix solutions containing the clay materials and (a) 10 % (b) 20 % CCR at 40±2 °C: K= Kamboinse, P= Pabre, Ko= Kossodo, S= Saaba.

The EC of all mixtures decreased over the curing time, at similar rate in the first 3 days, after which a clear difference was recorded for different clay materials and CCR contents (Fig. 10). For mixtures containing 10 % CCR, the clay materials from Saaba (S) and Kossodo (Ko) recorded the highest rate of decrease of EC compared to Kamboinse (K) and Pabre (P) between the 3rd and 14th day. This resulted in reaching the apparent minimum EC of about 2 mS/cm after 14 days of curing for Kossodo and Saaba and 28 days for Kamboinse and Pabre (Fig. 10a). For mixtures containing 20 % CCR, similar evolution of the EC was observed, the EC of Kamboinse and Pabre delayed until the 14th day before starting to decrease and reaching the apparent minimum value of about 2 mS/cm after 28 days (Fig. 10b). For both CCR contents, the EC can be considered to reach the minimum value after 28 days for all clay materials, given that no substantial decrease was recorded between the 28th and 45th day.

The decrease of the EC is explained by the consumption of Ca^{2+} and OH^- during the pozzolanic reaction of CCR with the clay materials [26,47]. In fact, linear correlation between the evolution of the EC and concentration of Ca^{2+} in mix solution of clay materials and CCR was previously reported [26]. The minimum EC in mix solutions can be related to the end of the consumption of Ca^{2+} and the occurrence of optimum maturity of the pozzolanic reaction. Thus clay materials from Kossodo and Saaba have better reactivity, given their early and high rate of consumption of Ca^{2+}, than the materials from Kamboinse and Pabre. The reactivity of clay materials from Saaba and Kossodo can respectively be related to their relatively high content and poorly ordered kaolinite as shown by XRD, TGA and FTIR (Section 3.4). The pozzolanic reaction involves aluminosilicate minerals such as kaolinite and eventually fine quartz from the clay materials and lime ($Ca(OH)_2$) from the CCR [19,26,29-30]. This is highly dependent on the particle fineness and content of reactive constituents and degree of order in their structure, with finer and poorly ordered materials presenting better reactivity [19,46].

3.5.2. Physico-mechanical performances of stabilized compressed earth blocks

Fig.11 presents the evolution of the average compressive strength of CEBs produced from clay materials from different sites stabilized with 0, 10, 20 % CCR. The average compressive strength of CEBs containing 0 % CCR (unstabilized/control) was 1.1 MPa for Kamboinse, 2 MPa for Pabre, 1.4 MPa for Kossodo and 0.8 MPa for Saaba (Table 4). The compressive strength of unstabilized CEBs is basically related to the cohesion behavior as well as the granular distribution of the clay materials. In fact, Pabre, which was characterized as highly cohesive material (Section 3.2), recorded the highest average compressive strength (2 MPa) compared to other sites which have medium cohesion. This suggests that only unstabilized clay material from Pabre are likely to produce ordinary CEBs for construction of single-storey (no load-bearing) building according to the ARS 674:1996 [21].

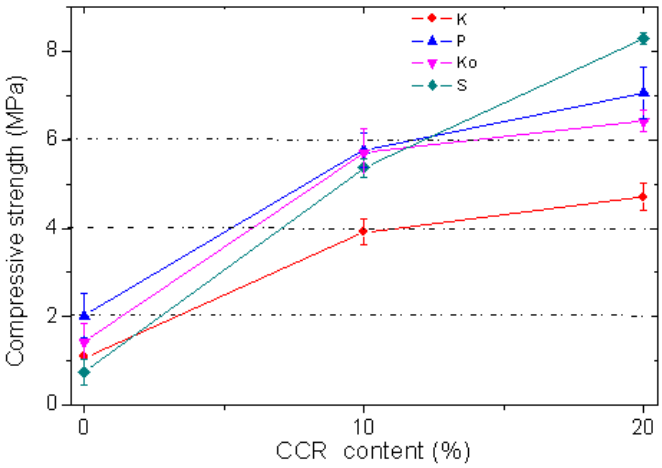

Fig.11. Dry compressive strength of CEBs made of clay materials from different sites stabilized with CCR cured for 45 days at 40±2 °C: K= Kamboinse, P= Pabre, Ko= Kossodo, S= Saaba.

The average compressive strength of the CEBs was substantially improved by stabilization with 10 % and 20 % CCR (Fig.11). The addition of 20 % CCR resulted in increasing the compressive strength, with respect to the control, more than 3.3 times (1.1 to 4.7 MPa) for Kamboinse, 2.6 times (2 to 7.1 MPa) for Pabre, 3.5 times (1.4 to 6.4 MPa) for Kossodo and 10 times (0.8 to 8.3 MPa) for Saaba (Table 4). Saaba not only recorded the highest compressive strength (8.3 MPa) after stabilization with 20 % CCR, but also the similar rate of improvement of the strength in the ranges of 0-10 % and 10-20 % CCR, contrary to other sites which presented little improvement beyond 10 % CCR (Fig.11). This suggests that the compressive strength of clay material from Saaba can further be improved by the addition of more than 20 % CCR while it would likely get to the optimum beyond 20 % CCR for other sites. Additionally, the average compressive strength of CEBs from Kossodo, Pabre and Saaba stabilized with 10 % CCR is greater than 4.5 MPa of the CEBs stabilized with 10 % geopolymer [25]. The compressive strength of CEBs from Saaba stabilized 20 % CCR is comparable to 8.5 MPa of CEBs stabilized 20 % geopolymer or 8-10 % cement [20,25].

The improvement of the compressive strength with the addition of CCR is related to the pozzolanic reaction between the clay materials and CCR. This reaction was previously responsible for the

formation of cementitious products such as CSH and CAH for binding the matrix of stabilized CEBs [24,26,44]. The reactivity of different clay materials (Section 3.5.1) is partly responsible for the difference in the improvement of the compressive strength of CEBs. Clay materials which recorded the highest rate of reaction (Saaba and Kossodo) recorded the highest rate of improvement of the compressive strength. Therefore, clay materials which would not fit for production of unstabilized CEBs can rather be used for production of stabilized CEBs.

Table 4. Physico-mechanical properties of stabilized CEBs produced from the investigated sites.

Clay material	CCR * content (wt %)	OWC ** (wt %)	Bulk density (kg/m^3)	Total void ratio (%)	Dry compressive strength (MPa)
Kamboinse	0	17	1800 (±12)	34.5 (±0.5)	1.1 (±0.4)
	10	19	1666 (±11)	38.8 (±0.4)	3.9 (±0.3)
	20	22	1624 (±9)	39.8 (±0.3)	4.7 (±0.3)
Pabre	0	16	1805 (±10)	32.1 (±0.6)	2.0 (±0.5)
	10	18	1729 (±5)	35.4 (±0.4)	5.8 (±0.4)
	20	20	1629 (±8)	38.0 (±0.3)	7.1 (±0.6)
Kossodo	0	13	2036 (±17)	30.0 (±0.8)	1.4 (±0.4)
	10	15	1892 (±15)	34.0 (±0.5)	5.7 (±0.5)
	20	17	1849 (±26)	34.6 (±0.9)	6.4 (±0.2)
Saaba	0	18	1646 (±15)	38.1 (±0.4)	0.8 (±0.3)
	10	20	1617 (±31)	38.8 (±1.2)	5.4 (±0.2)
	20	22	1613 (±9)	38.6 (±0.3)	8.3 (±0.1)

*CCR : Mass percent of CCR with respect to the dry mass of the clay material;
**OWC: Optimum water content, with respect to the dry mass of clay material + CCR, required for achieving the maximum dry density;
(…) Values in parentheses are the standard deviation.

Additionally, some physical properties such as bulk density and total void ratio can have impact on the mechanical performance of CEBs. Table 4 shows that the bulk density of CEBs stabilized with 0-20 % CCR ranges in 1800-1600 kg/m^3 for clay materials from other sites than Kossodo which has 2000-1800 kg/m^3. This is related to the optimum water content (OWC) required for achieving appropriate consistency for production of CEBs which increased between 16-22 %, except for Kossodo (13-17 %), with the addition of 0-20 % CCR. The increasing OWC with respect to the plasticity and fraction of fine particles of clay materials and addition of CCR resulted in increasing the apparent total void ratio in range of 32-40 % for the stabilized CEBs, except for Kossodo (30-34 %). The low OWC required for the material from Kossodo can be explained by

its lower content of fine particles (clay+silt) and higher content of gravel compared to other sites (Section 3.1). This is partly responsible for the relatively higher bulk density of CEBs produced from Kossodo. This high bulk density can also be related to the higher specific density (2.9) of the material from Kossodo compared to others (2.6-2.7).

The bulk density of CEBs stabilized with 10 % CCR is lesser than 1775 Kg/m^3 of CEBs stabilized with 10 % geopolymer or cement, except Kossodo [20,25]. This shows the structurally benefit of CCR-stabilized CEBs which can provide similar or better mechanical performance and lower dead load than cement-stabilized CEBs. Furthermore, the decrease of the bulk density of CEBs stabilized with CCR would potentially decrease their thermal conductivity and possibly contribute to the improvement of the thermal comfort in the building [10,25]. It is noteworthy that denser and lesser porous CEBs are more likely to have better durability such as the resistance to water absorption and erosion [7]. These results suggest that clay materials investigated from the four sites stabilized with 20 % CCR, cured for 45 days at 40±2 °C, can be used to produce ordinary CEBs suitable for construction of three-storey building except Kamboinse which is suitable for two-storey building [21]. This is regardless of whether the parameters of texture and plasticity of these clay materials fit in the boundaries recommended by the CRATerre. Nevertheless, further studies should be carried out for better understanding the long time durability and other engineering properties of these CEBs.

4. Conclusion

The suitability of clay materials from 4 different sites located in the vicinity of Ouagadougou in Burkina Faso was investigated for the production of CCR-stabilized CEBs. The characterization of the clay materials showed that Pabre and Kossodo respectively contain the highest (20-30 %) and the lowest (<10 %) fraction of clay particles. The material from Kamboinse behaves as medium to high plastic clay-silt, Pabre as medium plastic clay giving it high cohesion, Kossodo

475 as medium plastic clay-silt and Saaba as medium to high plastic silt. The material from Saaba
476 contains the highest fraction of clay minerals (60-75 %), mainly kaolinite, followed by Kamboinse
477 (45-75 %) while Pabre contains the highest fraction of quartz (45-60 %). Although Kossodo seems
478 to contain medium fraction of clay mineral (35-45%), different independent analyses suggested
479 that its kaolinite is poorly ordered than that of materials from the other sites. Moreover, the clay
480 materials from Kossodo as well as Saaba recorded the earliest and highest rate of reactivity with
481 CCR reaching the apparent maturity in 28 days of curing at 40±2 °C.

482 The relatively high cohesion of clay material from Pabre allows to produce unstabilized CEBs
483 which have the highest compressive strength (2 MPa) compared to Kamboinse (1.1 MPa),
484 Kossodo (1.4 MPa) and Saaba (0.8 MPa). Additionally, the compressive strength of CEBs
485 recorded improvement when they were stabilized with 20 % CCR reaching 7.1 MPa for Pabre,
486 4.7 MPa for Kamboinse, 6.4 MPa for Kossodo and 8.3 MPa for Saaba. The highest improvement
487 of the compressive strength of stabilized CEBs from Saaba and Kossodo was related to their
488 highest rate of reactivity with CCR. This reactivity can be related to the highest content and degree
489 of disorder of kaolinite in the clay materials from Saaba and Kossodo, respectively. In addition,
490 the clay material from Kossodo recorded the highest bulk density (2000-1800 kg/m^3) and void
491 ratio (30-34 %) related to its low plasticity and fraction of fine particles and high specific density
492 compared to other sites.

493 The results show that the clay materials from all studied sites stabilized with 20 % CCR are suitable
494 for production of stabilized CEBs with compressive strength of 4 MPa required for bearing load
495 in two-storey building. This suggests that clay materials which would not be suitable for
496 production of unstabilized CEBs can be suitable for production of CCR-stabilized CEBs. These
497 results also reveal that the selection of clay materials for production of CEBs based only on their
498 texture and plasticity may be misleading in leaving out the clay materials which would be suitable
499 considering their reactivity with the stabilizer. Nevertheless, more engineering and durability

properties, such as water absorption, compressive strength in saturated conditions and thermal properties, should be tested in order to better understand the performances of these CEBs in conditions of usage. Moreover, the study of technical feasibility should be carried on the viability of exploitation of the largest deposit (Kamboinse) whose volumetric quantity was estimated at 700 000 m^3.

Declaration of conflict of interest

None

Acknowledgement

Burkina Industrial Gas (BIG) provided the calcium carbide residue used in the present study free of charge. The first author acknowledges the contributions from Salif Kabore (2iE), Romain Wers, Frédéric Michel, François Fontaine and Frédéric Hatert (ULiège) throughout field works, laboratory characterizations and data analyses.

Funding

This work was supported by the "Académie de la Recherche et de l'Enseignement Supérieur" of the "Fédération Wallonie-Bruxelles (Belgium)-Commission de la Coopération au Développement (ARES-CCD) as part of an international research and development project "Amélioration de la qualité de l'habitat en terre crue au Brukina Faso-*Improving the quality of earth-based housing in Burkina Faso, PRD*2016-2021".

References

[1] N. a. Nzeugang, M.R. Eko, N. Fagel, K. V. Kabeyene, a. Njoya, B. a. Madi, J.R. Mache, M.U. Chinje, Characterization of clay deposits of Nanga-Eboko (central Cameroon): suitability for the production of building materials, Clay Miner. 48 (2013) 655–662. doi:10.1180/claymin.2013.048.4.18.

[2] A. Nkalih Mefire, A. Njoya, R.Y. Fouateu, J.R. Mache, N.A. Tapon, A.N. Nzeugang, U.M. Chinje, P.Pilate, P.Flament, S. Siniapkine, A. Ngono, N.Fagel, Occurrences of kaolin in Koutaba (west Cameroon):

Mineralogical and physicochemical characterization for use in ceramic products, Clay Miner. 50 (2015) 593–606. doi:10.1180/claymin.2015.050.5.04.

[3] H. El Boudour El Idrissi, L. Daoudi, M. El Ouahabi, A. Balo Madi, F. Collin, N. Fagel, Suitability of soils and river deposits from Marrakech for the manufacturing of earthenware, Appl Clay Sci. 129 (2016) 108–115. doi:10.1016/j.clay.2016.05.013.

[4] B. Abdelmalek, B. Rekia, B. Youcef, B. Lakhdar, N. Fagel, Mineralogical characterization of Neogene clay areas from the Jijel basin for ceramic purposes (NE Algeria -Africa), Appl Clay Sci. 136 (2017) 176–183. doi:10.1016/j.clay.2016.11.025.

[5] D. Tsozué, A.N. Nzeugang, J.R. Mache, S. Loweh, N. Fagel, Mineralogical, physico-chemical and technological characterization of clays from Maroua (Far-North, Cameroon) for use in ceramic bricks production, J Build Eng. 11 (2017) 17–24. doi:10.1016/j.jobe.2017.03.008.

[6] H.B. Nagaraj, M.V. Sravan, T.G. Arun, K.S. Jagadish, Role of lime with cement in long-term strength of Compressed Stabilized Earth Blocks, Int J Sustain Built Environ. 3 (2014) 54–61. doi:10.1016/j.ijsbe.2014.03.001.

[7] J.A. Bogas, M. Silva, M. da G. Gomes, Unstabilized and stabilized compressed earth blocks with partial incorporation of recycled aggregates of recycled aggregates, Int J Archit Herit. 3058 (2018) 1–16. doi:10.1080/15583058.2018.1442891.

[8] A.A. Shubbar, M. Sadique, P. Kot, W. Atherton, Future of clay-based construction materials – A review, Constr Build Mater. 210 (2019) 172–187. doi:10.1016/j.conbuildmat.2019.03.206.

[9] G.M. Reeves, I. Sims, J.C. Cripps, Clay Materials Used in Construction, Geology Society of London, London, 2006.

[10] H.S. Moussa, P. Nshimiyimana, C. Hema, O. Zoungrana, A. Messan, L. Courard, Comparative Study of Thermal Comfort Induced from Masonry Made of Stabilized Compressed Earth Block vs Conventional Cementitious Material, J Miner Mater Charact Eng. 7 (2019) 385–403. doi:10.4236/jmmce.2019.76026.

[11] C.M. Hema, G. Van Moeseke, A. Evrad, L. Courard, A. Messan, Vernacular housing practices in Burkina Faso: Representative models of construction in Ouagadougou and walls hygrothermal efficiency, in: Energy Procedia, Elsevier, 2017: pp. 535–540. doi:10.1016/j.egypro.2017.07.398.

[12] A.L. Murmu, A. Patel, Towards sustainable bricks production: An overview, Constr Build Mater. 165 (2018) 112–125. doi:10.1016/j.conbuildmat.2018.01.038.

[13] INSD, Annuaire statistique 2016, Institut national de la statistique et de la démographie, Ouagadougou, Burkina Faso, 2017.

555 [14] U. Wyss, La construction en « matériaux locaux » état d'un secteur à potentiel multiple. Direction du
556 Développement et de la Coopération Suisse, Ouagadougou, Burkina Faso, 2005.
557 [15] J. Cid-Falceto, R.F. Mazarron, I. Canas, Assessment of compressed earth blocks made in Spain: International
558 durability tests, Constr Build Mater. 37 (2012) 738–745.
559 [16] H. Houben, H. Guillaud, CRATerre: Traité de Construction en Terre: L'encyclopédie de la construction en
560 terre, Vol. I, Editions Parathèses, Marseille, 2006.
561 [17] J.C. Morel, A. Pkla, P. Walker, Compressive strength testing of compressed earth blocks, Constr Build Mater.
562 21 (2007) 303–309. doi:10.1016/j.conbuildmat.2005.08.021.
563 [18] M.C.J. Delgado, I.C. Guerrero, The selection of soils for unstabilised earth building: A normative review,
564 Constr Build Mater. 21 (2007) 237–251. doi:10.1016/j.conbuildmat.2005.08.006.
565 [19] S. Diamond, J.L. White, W.L. Dolch, Transformation of Clay Minerals by Calcium Hydroxide Attack, in:
566 Twelfth Natl Conf Clays Clay Miner, 1963: pp. 359–379. doi:10.1346/CCMN.1963.0120134.
567 [20] P. Walker, T. Stace, Properties of some cement stabilised compressed earth blocks and mortars, Mater Struct
568 Constr. 30 (1997) 545–551. doi:10.1007/BF02486398.
569 [21] CDI, CRATerre-EAG, Compressed Earth Blocks: Standards guide-Technology series N° 11, CDI (ARSO),
570 Brussels-Belgium, 1998.
571 [22] B.V. Venkatarama Reddy, S.R. Hubli, Properties of lime stabilised steam-cured blocks for masonry, Mater
572 Struct. 35 (2002) 293–300. doi:10.1007/BF02482135.
573 [23] P.J. Walker, Strength and Erosion Characteristics of Earth Blocks and Earth Block Masonry, J Mater Civ Eng.
574 16 (2004) 497–506. doi:10.1061/(ASCE)0899-1561(2004)16:5(497).
575 [24] P. Nshimiyimana, D. Miraucourt, A. Messan, L. Courard, Calcium Carbide Residue and Rice Husk Ash for
576 improving the Compressive Strength of Compressed Earth Blocks, MRS Adv. 3 (2018) 2009–2014.
577 http://hdl.handle.net/2268/226552.
578 [25] O.S. Sore, A. Messan, E. Prud'homme, G. Escadeillas, F. Tsobnang, Stabilization of compressed earth blocks
579 (CEBs) by geopolymer binder based on local materials from Burkina Faso, Constr Build Mater. 165 (2018)
580 333–345. doi:10.1016/j.conbuildmat.2018.01.051.
581 [26] P. Nshimiyimana, A. Messan, Z. Zhao, L. Courard, Chemico-microstructural changes in earthen building
582 materials containing calcium carbide residue and rice husk ash, Constr Build Mater. 216C (2019) 622–631.
583 doi:https://doi.org/10.1016/j.conbuildmat.2019.05.037.
584 [27] A. Al-Fakih, B.S. Mohammed, M.S. Liew, E. Nikbakht, Incorporation of waste materials in the manufacture
585 of masonry bricks: An update review, J Build Eng. 21 (2019) 37–54. doi:10.1016/j.jobe.2018.09.023.

[28] S. Masuka, W. Gwenzi, T. Rukuni, Development, engineering properties and potential applications of unfired earth bricks reinforced by coal fly ash, lime and wood aggregates, J Build Eng. 18 (2018) 312–320. doi:10.1016/j.jobe.2018.03.010.

[29] W. Mechti, T. Mnif, B. Samet, M.J. Rouis, Effect of the secondary minerals on the pozzolanic activity of calcined clay: case of quartz, IJRRAS. 12 (2012) 61–71. doi:10.1684/bdc.2011.1430.

[30] D. Ciancio, C.T.S. Beckett, J.A.H. Carraro, Optimum lime content identification for lime-stabilised rammed earth, Constr Build Mater. 53 (2014) 59–65. doi:10.1016/j.conbuildmat.2013.11.077.

[31] M. Al-Mukhtar, S.A.A. Khattab, J.-F. Alcover, Micorstructure and geotechnical properties of lime treated expansive soil, Eng Geol. 139–140 (2012) 17–27. doi:10.1061/(ASCE)0899-1561(2007)19:4(358).

[32] NF EN ISO 17892-4, Geotechnical investigation and testing - Laboratory testing of soil - Part 4 : Determination of particle size distribution, AFNor, Saint-Denis La Plaine Cedex, 2018.

[33] NF P 94-051, Sols: reconnaissance et essais-Détermination des limites d'Atterberg-Limite de liquidité à la coupelle-Limite de plasticité au rouleau, AFNor, Saint-Denis La Plaine Cedex, 1993.

[34] NF EN 1097-6, Essais pour déterminer les caractéristiques mécaniques et physiques des granulats - Partie 6 : détermination de la masse volumique réelle et du coefficient d'absorption d'eau, Saint-Denis La Plaine Cedex, 2014.

[35] NF P94-093, Sols : reconnaissance et essais - Détermination des références de compactage d'un matériau - Essai Proctor Normal - Essai Proctor modifié, AFNor, Saint-Denis La Plaine Cedex, 2014.

[36] H.E. Cook, P.D. Johnson, J.C. Matti, I. Zemmels, Methods of sample preparation and x-ray diffraction data analysis, x-ray mineralogy laboratory, in: D.E. Hayes, L.A. Frakes (Eds.), Init Repts DSDP, U.S. Govt. Printing Office, Washington, 1975: pp. 999–1007.

[37] T. Boski, J. Pessoa, P. Pedro, J. Thorez, J.M.A. Dias, Factors governing abundance of hydrolyzable amino acids in the sediments from the N . W . European Continental Margin (47-50 °N), Prog Oceanogr. 42 (1998) 145–164.

[38] N. Fagel, T. Boski, L. Likhoshway, H. Oberhaensli, Late Quaternary clay mineral record in Central Lake Baikal (Academician Ridge, Siberia), Palaeogeogr Palaeoclimatol Palaeoecol. 193 (2003) 159–179. doi:10.1016/S0031-0182(02)00633-8.

[39] M. Földvári, Handbook of the thermogravimetric system of minerals and its use in geological practice, Hungarian Academy of Sciences, Budapest, 2011. doi:10.1556/CEuGeol.56.2013.4.6.

[40] J. Yvon, O. Lietard, J.M. Cases, J.F. Delon, Minéralogie des argiles kaoliniques des Charentes, Bull Minéralogie. 105 (1982) 431–437.

[41] CDE, CRATerre-EAG, ENTPE, Compressed earth blocks: testing procedures guide-Technology series N° 16, CDE (ARSO), Brussels-Belgium, 2000.

[42] XP P 13-901, Blocs de terre comprimée pour murs et cloisons, Définitions-Spécifications-Méthodes d'essais-Conditions de réception, AFNor, Saint-Denis La Plaine Cedex, 2001.

[43] B. Lorentz, N. Shanahan, Y.P. Stetsko, A. Zayed, Characterization of Florida kaolin clays using multiple-technique approach, Appl Clay Sci. 161 (2018) 326–333. doi:10.1016/j.clay.2018.05.001.

[44] M. Al-Mukhtar, S. Khattab, J.F. Alcover, Microstructure and geotechnical properties of lime-treated expansive clayey soil, Eng Geol. 139–140 (2012) 17–27. doi:10.1016/j.enggeo.2012.04.004.

[45] C. Bich, J. Ambroise, J. Péra, Influence of degree of dehydroxylation on the pozzolanic activity of metakaolin, Appl Clay Sci. 44 (2009) 194–200. doi:10.1016/j.clay.2009.01.014.

[46] A. Tironi, M.A. Trezza, A.N. Scian, E.F. Irassar, Kaolinitic calcined clays: Factors affecting its performance as pozzolans, Constr Build Mater. 28 (2012) 276–281. doi:10.1016/j.conbuildmat.2011.08.064.

[47] M. Al-Mukhtar, A. Lasledj, J.-F. Alcover, Behaviour and mineralogy changes in lime-treated expansive soil at 50°C, Appl Clay Sci. 50 (2010) 199–203. doi:10.1016/j.clay.2010.07.022.